PHYSICAL REVIEW C VOLUME 27, NUMBER 2 FEBRUARY 1983

Ground-state photoneutron reactions in ^{15}N

J. D. Watson, J. W. Jury, and P. C-K. Kuo
Department of Physics, Trent University, Peterborough, Ontario, Canada K9J 7B8

W. F. Davidson and N. K. Sherman
Physics Division, National Research Council of Canada, Ottawa, Ontario, Canada K1A 0R6

K. G. McNeill
Department of Physics, University of Toronto, Toronto, Ontario, Canada M5S 1A7

(Received 8 October 1982)

Photoneutron angular distributions were measured by time-of-flight techniques for the reaction $^{15}N(\gamma,n_0)^{14}N$ over the region of excitation energy from 15 to 25 MeV. Ground state cross sections were obtained by stepping the bremsstrahlung end point over the energy region of interest in 2 MeV intervals. By fitting the spectral data to a series of Legendre polynomials, angular distribution coefficients were extracted and interpreted on the basis of a simple single particle model. It appears that a large fraction of the photoabsorption strength leading to decays via the ground state channel is due to the formation of $J^\pi=\frac{3}{2}^+$, $T=\frac{1}{2}$ states in ^{15}N which decay by d-wave neutron emission. The data support an approximation of purely electric dipole absorption in the region measured. Some small amount of s-wave neutron emission interfering with the dominant $p_{1/2}\rightarrow d_{3/2}$ transition is consistent with an observed value for the a_2/a_0 coefficient of -0.7 ± 0.2. The (γ,n_0) cross section integrated between threshold and 30 MeV is estimated to represent about one-third of the total strength in the neutron channel. A state identified at 17.3 MeV is consistent in energy and composition with a theoretical prediction based on a shell model calculation using a residual interaction with a Soper mixture of exchange forces.

[NUCLEAR REACTIONS $^{15}N(\gamma,n_0)$, $E_\gamma=15$–25 MeV; measured differential cross sections as function of angle; extracted Legendre coefficients; estimated s/d matrix-element ratio in dipole approximation.]

I. INTRODUCTION

The completely filled valence p shells of the neutron and proton wells in ^{16}O make it a spherically symmetric nucleus and therefore an ideal test case for modern continuum shell-model calculations (see Refs. 1–3) which attempt to describe more complex nuclei in terms of a particle or hole which is weakly coupled to a symmetrical core. The polarizability of nuclei which can be described in this way should be determined primarily by the nature of the core. Therefore, one would expect ^{16}O and its neighbors in the Periodic Table to exhibit similarities in their photoabsorption cross section.

Photoparticle reactions in the region of the giant dipole resonance (GDR) can be understood in terms of collective absorption together with the interaction between a single particle and a hole state in the residual nucleus. But, as is generally the case, the GDR is too complex and the states are too broad and overlapping to observe individual single particle transitions.

The ground states of ^{17}O and ^{15}N have isospin $T=\frac{1}{2}$. The photon absorption cross section for these nuclei can be split into $T_>$ ($\Delta T=1$) and $T_<$ ($\Delta T=0$) components, with part of the $T_<$ component forming a pygmy resonance at an energy below the GDR. It is in this region that narrow resonances can be identified in both these nuclei.

Several theories predict the single particle composition of states at these energies[4–7] but relatively little experimental data on these nuclei exist[8–10] which fully elucidate the single particle nature of these states. The measurement of the angular distribution of photoneutrons from the reaction $^{15}N(\gamma,n_0)^{14}N$ reported here gives insight into the single particle composition of the low lying states. In particular, a resonance at 17.3 ± 0.1 MeV excitation energy which appears in a recent measurement of the total photoneutron cross section[11] provides a basis for testing

the various residual interactions used in the calculations. This is facilitated by the fact that the ground state photoneutron channel must be exclusively $T_<$ because the $T_>$ states are isospin forbidden to decay to a $T=0$ daughter by neutron emission.

Wender *et al.*[12] have recently measured the cross section and angular distribution of photons for the inverse reaction ^{14}N$(n,\gamma_0)^{15}$N and obtained the corresponding photoexcitation cross section by detailed balance. However, they reported angular distributions at only seven excitation energies leaving the need for a higher resolution measurement over a wider energy range.

A comparison of our measured ground-state cross section with the (γ,n_{tot}) cross section of Ref. 11 shows the fraction of strength in the photoneutron channel which is taken up by ground state transitions alone. The branching ratio information can be used to test theories predicting the composition of states in the $T_<$ pygmy resonance of ^{15}N.

II. EXPERIMENTAL DETAILS

Figure 1 shows the experimental facility in the X-Ray and Nuclear Radiation section of the National Research Council of Canada (NRCC) which was used to measure multiangle neutron energy spectra using time-of-flight techniques. The apparatus is the same as that described in detail by Jury *et al.*[13] and consequently only the salient features are outlined below.

Bremsstrahlung was produced by electrons from the NRCC linear accelerator impinging on an 0.8 mm tantalum radiator. The linac delivered electron bursts of 1 A of current and 6 ns duration at 720 Hz. Time-of-flight spectra were recorded at 8 angles simultaneously over 10 m flight paths. Using a CAMAC data acquisition system, each detector produced a "stop" pulse for its own time digitizer [time-to-digital converter (TDC)], which was previously started by the photon beam striking a detector near the sample. Up to 7 cm of bismuth was placed in the flight paths to help reduce the intensity of gamma flash in the detectors. A computer-controlled target wheel cycled the photoneutron samples into the beam at 60 s intervals. This process was carried on for the duration of a measurement which usually consisted of 300 cycles of the target wheel and helped to ensure uniform irradiation of the samples. Measurements were taken at five different end point energies between 18 and 26 MeV since only neutrons within the first 2.3 MeV of the highest possible energy could be unambiguously associated with ground state transitions at a given end point energy.

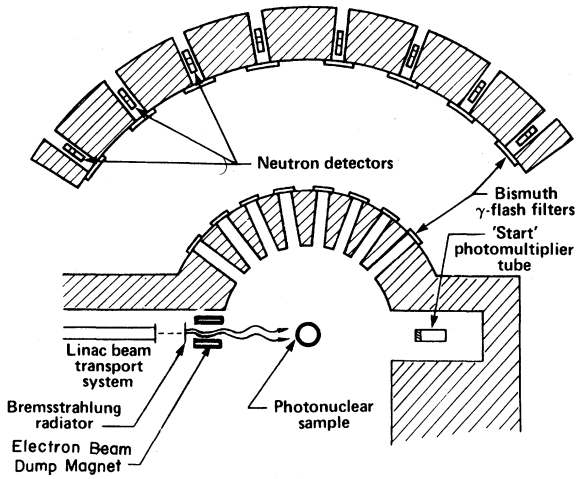

FIG. 1. Schematic diagram of the facility for the measurement of photoneutron angular distributions at the Linear Accelerator Laboratory of the National Research Council of Canada. Shown are the eight 10-m flight paths and associated shielding.

Data from a total of four photoneutron samples were recorded at each end point energy. These were D_2O, H_2O, $(^{15}NH_3)_2SO_4$, and a background target. The sample materials were contained in cylindrical containers of an annular design with a thickness of 0.8 cm and diameter of 5.6 cm. The sample holders were constructed from extruded acrylic tubing which was machined to a thickness of 0.625 mm. The finished containers weighed only 23 g [compared to the 135 g of the $(^{15}NH_3)_2SO_4$] and contributed negligibly to the background in the experiment. The design was facilitated by a computer code which compared the self-scattering of neutrons by the target for various thicknesses of solid and annular cylinders.

The ^{15}N sample was in the form of 135 g of ammonium sulphate which was 98% $(^{15}NH_3)_2SO_4$ giving 30 g of ^{15}N isotope. The background target was made up to contain the same amount of sulphur and oxygen present in the ammonium sulphate. Because the Q values for the photoneutron reactions in ^{32}S and ^{16}O are -15.1 and -15.6 MeV, respectively, and the Q value for ^{15}N is -10.8 MeV, any background photoneutrons from the oxygen and sulphur in the sample were kinematically separated from the ^{15}N photoneutrons by about 4.3 MeV.

The relative efficiency of the detectors was obtained in the same manner as previously reported[13] by employing a very thin radiator ($\sim$0.2 mm thick titanium radiator), by assuming a thin-target Schiff spectrum of photons, and by using the deuteron photodisintegration cross section calculated by Fabian and Arenhovel[14] at low energies ($E_\gamma < 10$ MeV) and by Partovi[15] at higher energies.

III. DATA ANALYSIS AND ESTIMATION OF UNCERTAINTIES

The major source of error in this experiment was the statistical error associated with the raw time-of-flight data, this being on the order of $\pm 0.5\%$. The small amount of expensive ^{15}N isotope (30 g) which was available for this experiment made further reduction of this uncertainty too costly and time consuming. The raw time-of-flight data were processed to the stage of differential photoneutron cross sections by means of the following steps.

A. Dead time correction

Each time-of-flight spectrum was corrected for dead time of the appropriate detector. The problem of dead time arose from the fact that the time digitizer associated with each detector could register only one stop per start, which represented in this case a maximum of 720 events per second. Therefore, the possibility existed that should the count rate approach about 10% or more of this limit, an appreciable number of neutrons would go undetected. Although the ^{15}N count rate was usually 60 times less than this limit, a dead time correction was applied to the data in all cases.

B. Beam independent background

A small background, independent of accelerator beam intensity, was observed to underlie the time-of-flight spectra. It was associated with cosmic rays and natural background radiation from nearby shielding material. It made up about 3% of the counts in the time channels of interest in this experiment. This background was removed from the data by averaging counts in regions of the time-of-flight spectra which were kinematically separated from the region of neutron events produced by the samples. This level was then subtracted from the entire spectrum. The error introduced by this procedure is estimated to be less than 1%.

C. Subtraction of beam dependent backgrounds

The neutron spectra from both the heavy water and the ammonium sulphate samples contained foreground and background components. The backgrounds were due to the contaminants present in each sample: oxygen in the case of D_2O and sulphur and oxygen in the case of $(^{15}NH_3)_2SO_4$, in addition to various elements in the low mass sample containers (mainly carbon).

The backgrounds associated with each sample were measured separately and then subtracted from the foreground and background spectra. The relative irradiation times between foreground and background were chosen to minimize the statistical error associated with the subtraction.

In the excitation energy region of interest (15–26 MeV) the foreground (topmost 2.3 MeV neutrons) was kinematically separated from the background because of the relatively low Q value of ^{15}N (-10.8 MeV) and the background was very small, typically less than 10% of the foreground. Therefore, the error associated with this subtraction (statistical and systematic) is estimated to be less than 1%.

D. Conversion to energy spectra

The time-of-flight data were converted to energy spectra using relativistically exact relationships between excitation energy and neutron energy, neutron energy and flight-time, laboratory and center-of-mass scattering angle, and solid angle and center-of-mass velocity. The data were then corrected by the detector efficiency to give neutron spectra in terms of excitation energy in the center of mass. The resolution widths used in the conversion to energy spectra were chosen to approximate the energy-dependent experimental resolution inherent in time-of-flight measurements.

The accuracy of the conversion to energy spectra depended upon the accuracy of the time calibration of the system. For this reason, the calibration was carried out using two methods. First, correlations between flight time (for a 10 m flight path) and neutron energy were made using as a reference several easily identified neutron absorption resonances in the ^{12}C neutron scattering cross section and several narrow peaks in the ^{16}O photoneutron cross section. This technique produced a calibration up to neutron energies of 8 MeV which was accurate to about 1%. Next, photon spectra were derived from the deuterium data at each angle at several of the bremsstrahlung end point energies used. By a close inspection of the energy of the end point of each bremsstrahlung spectrum, additional refinements were made to the calibration. Thus the calibration of the system was determined to less than 1% up to neutron energies of 12 MeV.

E. Extraction of the cross section

The cross section for the reaction $^{15}N(\gamma,n_0)^{14}N$ was calculated relative to the theoretical photodisintegration cross section for ^2H (Refs. 14 and 15) using the relationship:

$$\left[\frac{d\sigma}{d\Omega}\right]_{^{15}\mathrm{N}}(E_\gamma,\theta)=\frac{\mathrm{Events}_{^{2}\mathrm{N}}(E_\gamma,\theta)}{\mathrm{Events}_{^{2}\mathrm{H}}(E_\gamma,\theta)}\frac{\phi_{^{2}\mathrm{H}}(E_\gamma)}{\phi_{^{15}\mathrm{N}}(E_\gamma)}\times\frac{\eta_{^{2}\mathrm{H}}(E_n,\theta)}{\eta_{^{15}\mathrm{N}}(E_n,\theta)}\frac{N_{^{2}\mathrm{H}}}{N_{^{15}\mathrm{N}}}\times\left[\frac{d\sigma}{d\Omega}\right]_{^{2}\mathrm{H}}(E_\gamma,\theta)\,, \tag{1}$$

where the ratio of the solid angle factors has been omitted (~ 1) and ϕ is the photon flux, η is the detector efficiency, N is the number of target nuclei, and the number of events is expressed as

$$\mathrm{Events}=\int_{E_\gamma-\Delta E_\gamma/2}^{E_\gamma+\Delta E_\gamma/2} n(E_\gamma,\theta)dE_\gamma\simeq\tilde{n}\Delta E_\gamma\,, \tag{2}$$

where $n(E_\gamma,\theta)$ is the product of the photon flux and the cross section, $\tilde{n}$ is the mean value of this product over the energy region specified, and ΔE_γ is the resolution width of the photon energy bin used.

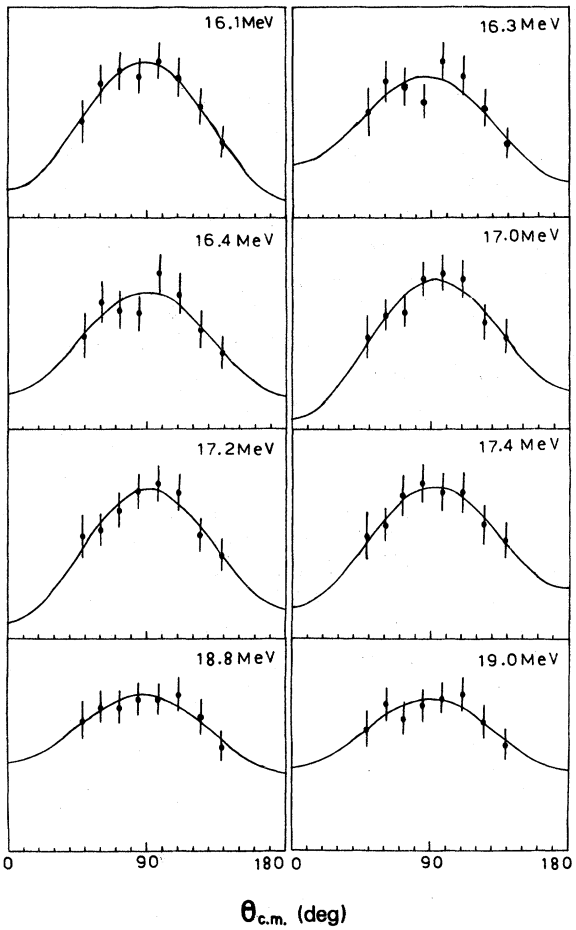

FIG. 2. Shown are sample experimental raw data and second-order fits to a series of Legendre polynomials. Error bars represent statistical uncertainties only.

The photon flux in each sample canceled because the targets were cycled to ensure uniform irradiation (to within about 0.5%). The fact that each sample received equal amounts of radiation was verified by a continuous monitoring of the charge deposited on the electron dump block.[13] The uncertainty associated with the above method of calculation is estimated to be of the order of the statistical accuracy associated with each point. However, any future modifications in the theoretical cross section for ^{2}H will affect this cross section scale directly.

F. Extraction of the anisotropy coefficients

The angular distribution of photoneutrons at each excitation energy was fitted by a series of Legendre polynomials

$$W(\theta)=\sum_{l=0}^{3}a_l P_l(\cos\theta)\,, \tag{3}$$

where $W(\theta)$ is the yield at angle θ in the c.m. frame. The fitting technique followed that described by Bevington.[16] Figure 2 shows eight sample fits. The errors shown are statistical errors only. In each case the reduced χ^2 associated with the fit was observed

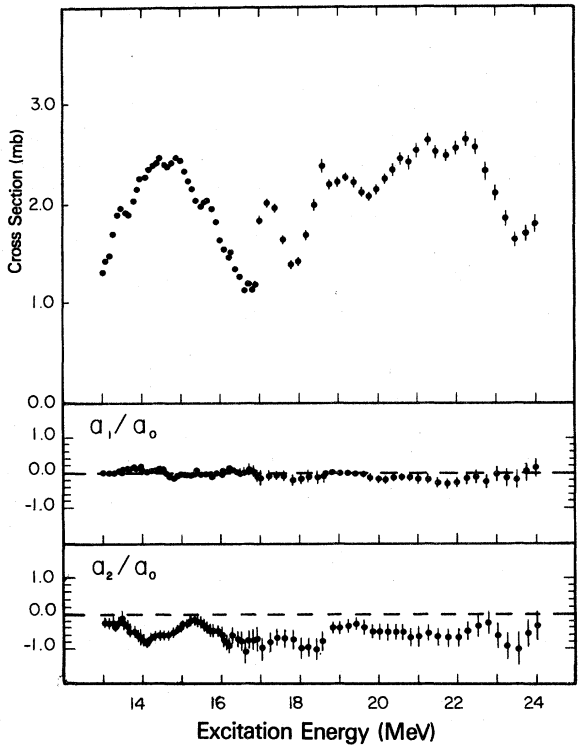

FIG. 3. The cross section for the reaction $^{15}\mathrm{N}(\gamma,n_0)^{14}\mathrm{N}$ is shown along with the normalized anisotropy coefficients, a_1/a_0 and a_2/a_0 as functions of excitation energy. The scale of the cross section was determined relative to that of the deuteron.

to be ~ 1 for fits to third order [up to $P_3(\cos\theta)$]. The magnitude of the statistical uncertainty associated with the data precluded a fit to higher order.

The a_0 coefficient measures the degree of isotropy of the distribution and gives an average value for the differential cross section over the angular range of the data. The higher order coefficients reflect the anisotropic and asymmetric character of the distribution.

IV. RESULTS

The normalized a_3/a_0 coefficient was observed to be zero in all cases (within the accuracy of this measurement). Therefore a fit to second order was made and used to calculate a_0, a_1, and a_2. The a_0 coefficient and the normalized a_l coefficients are shown in Fig. 3. The quantity $4\pi a_0$ represents the total ground state cross section integrated over solid angle.

The figure is composed of five independent measurements of the cross section at different bremsstrahlung end point energies. The data lying in the uppermost energy region within 500 keV of each end point contained too few events to justify a Legendre fit and were discarded. The ground state cross section is composed of 2.3 MeV segments taken from below the effective end point of each measurement.

The a_0 coefficient shows considerable structure. In particular, a reasonably sharp peak between 17 and 18 MeV is suggestive of a resonance of single particle character. Although the ground state cross section shows considerable strength in the region below 19 MeV, there is little evidence of the giant dipole resonance reported[11] to be centered at 23 MeV. Above 18 MeV, the cross section ($4\pi a_0$) remains close to a value of 2 mb, while the (γ,n_{tot}) strength in this region climbs to 12 mb.

The normalized a_1/a_0 coefficient, which represents the amount of $E1\cdot M1$ and $E1\cdot E2$ interference in the photoabsorption matrix element for the reaction, is seen to be zero over most of the region of this measurement. However, a deviation from zero to a minimum value of -0.3 ± 0.2 at 21.75 MeV is noted.

The normalized a_2/a_0 coefficient spans a wide range of values between 0.0 and -1.0. There are regions where both the a_1/a_0 and a_2/a_0 coefficients are close to zero and a high degree of isotropy is present in the angular distribution.

Minima in the a_2/a_0 coefficients correspond to a peaking of the cross section at 90°. These minima are present at excitation energies of 14, 16–18.4, and 23.5 MeV. The error bars shown in Fig. 3 are fitting errors.

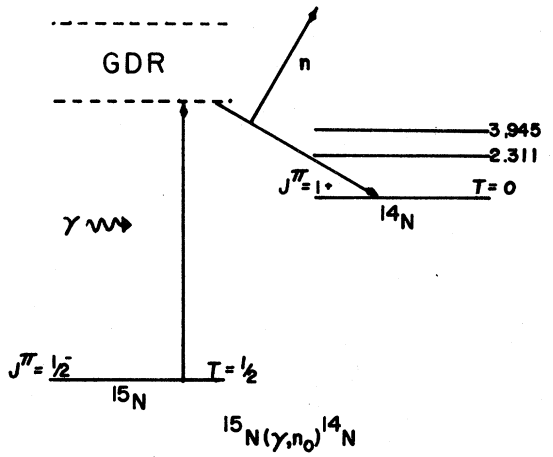

FIG. 4. A schematic representation of the reaction $^{15}N(\gamma,n_0)^{14}N$. Photoneutrons emitted in transitions to the ground state lie in the energy region within 2.3 MeV of the maximum possible neutron energy. Although the total photoneutron reaction, $^{15}N(\gamma,n_{\text{tot}})^{14}N$, can proceed via both $T_<$ and $T_>$ intermediates in ^{15}N, the ground state reaction is restricted to transitions involving only $T_<$ states.

V. DISCUSSION

The $^{15}N(\gamma,n_0)^{14}N$ reaction is illustrated schematically in Fig. 4. Dipole absorption of a photon by the ground state of ^{15}N ($J^\pi=\frac{1}{2}^-$) leads to the formation of an excited state ($J^\pi=\frac{1}{2}^+$, or $J^\pi=\frac{3}{2}^+$) which decays by neutron emission to the ground state of ^{14}N. The ground state of ^{15}N has $T=\frac{1}{2}$ and the ground state of ^{14}N has $T=0$. Since the neutron can carry off only $\frac{1}{2}$ unit of isospin, the photoabsorption resulting in transitions to the ground state

TABLE I. Expressions for the a_0 and a_2 coefficients extracted from a fit of series of Legendre polynomials to the angular distribution of neutrons are given in terms of electric dipole matrix elements. The matrix elements are expressed in the form $E1(l,J,s)$, where l is the orbital angular momentum of the emitted particle, J is the angular momentum of the intermediate excited state, and s is the channel spin.

$$a_0=2E1(0,\tfrac{1}{2},\tfrac{1}{2})^2+2E1(2,\tfrac{1}{2},\tfrac{3}{2})^2+4E1(2,\tfrac{3}{2},\tfrac{1}{2})^2$$
$$+4E1(0,\tfrac{3}{2},\tfrac{3}{2})^2+4E1(2,\tfrac{3}{2},\tfrac{3}{2})^2$$

$$a_2=-2.83E1(2,\tfrac{1}{2},\tfrac{3}{2})E1(2,\tfrac{3}{2},\tfrac{3}{2})\cos\delta_1$$
$$-4.00E1(0,\tfrac{1}{2},\tfrac{1}{2})E1(2,\tfrac{3}{2},\tfrac{1}{2})\cos\delta_2$$
$$+2.83E1(2,\tfrac{1}{2},\tfrac{3}{2})E1(0,\tfrac{3}{2},\tfrac{3}{2})\cos\delta_3$$
$$-2.00E1(2,\tfrac{3}{2},\tfrac{1}{2})^2$$

TABLE II. Breakdown of the ground state cross section into single particle transitions based on a simple case study of the ratio a_2/a_0 expressed in terms of transition matrix elements. s-wave neutrons are produced by the transitions $p_{1/2}{}^{-1}s_{1/2}$; d-wave by $p_{1/2}{}^{-1}d_{3/2}$ transitions.

Energy (MeV)	Single-particle strength	Energy (MeV)	Single-particle strength
13–14	s	19	d ($s=0.4d$)
14–14.7	d	20–22	d
14.7–15.7	s	23	s
16–19	d ($s=0.4d$)	23+	d

of ^{14}N can proceed only through $T_{1/2}$ ($T_<$) states in the excited ^{15}N system, whereas the total photoneutron reaction can proceed via both $T=\frac{1}{2}$ and $T=\frac{3}{2}$ states.

However, although transitions to the ground state are exclusively $T_<$, they do not necessarily exhaust all the $T_<$ strength in the GDR. Transitions to $T=0$ excited states in ^{14}N may also take place; these are not measured in this ground state experiment. That the above reaction model (an electric dipole approximation) is valid is substantiated by the observation that the a_1/a_0 coefficient is near zero, indicating that the absorption process is mainly dipole in nature.

Table I gives the expansion of the a_0 and a_2 coefficients in terms of electric dipole transition matrix elements[17] in the channel spin representation. Even in the dipole approximation, the analysis is complex and in the absence of information on the relative phase shifts involved, or measurements of photoneutron polarizations, a rigorous treatment is impossible. However, further analysis is greatly facilitated by examining the following special cases:

(i) No s-wave neutrons are emitted; all transitions are $p_{1/2}{}^{-1}d_{3/2}$ single particle excitations. In this case one expects a value of $a_2/a_0=-0.5$.

(ii) No d-wave neutrons; all transitions are $p_{1/2}{}^{-1}s_{1/2}$ single particle excitations. For this case, $a_2/a_0=0$.

(iii) Intermediate case; some small amount of s wave is mixed with mostly d-wave transitions. With a ratio of amplitudes $s/d=0.3$ (i.e., $\sigma_s\sim 10\%$ of σ_d) values of $a_2/a_0\sim -0.7$ (observed in the data) can be obtained under the simple assumption of channel spin $\frac{1}{2}$ dominance and $\cos\delta_2=+1$ (see Table I).

Table II shows a breakdown of the ground state cross section into single particle transitions based on the above analysis of the a_2/a_0 coefficient. The state at 17.3 MeV excitation seems to be primarily the result of a $p_{1/2}{}^{-1}d_{3/2}$ transition with some admixture of $p_{1/2}{}^{-1}s_{1/2}$ strength acting to lower its a_2/a_0 value from -0.5 to -0.7.

A comparison of our data with a recent shell model study of the GDR in ^{15}N by Albert *et al.*[18] is shown in Fig. 5. The calculation assumes a residual interaction in the form of a δ-function potential which employs a Soper mixture of exchange forces. The theoretical result represents the cross section for all reaction channels with $\Delta T=0$. The ordinate scale of the calculated curve has been divided by a factor of 4 to facilitate a comparison with the (γ,n_0) results. Below 17 MeV, the experimental (γ,n_0) cross section represents about half the predicted total photoabsorption strength, which one would expect since ground state transitions dominate the neutron channel in this region of excitation energy and, because the (γ,n_0) and (γ,p_0) Q values are near-

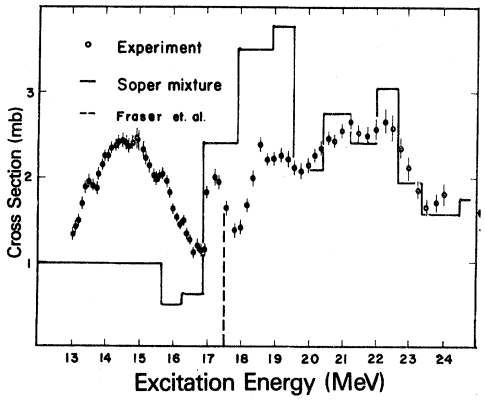

FIG. 5. A comparison of the measured cross section is made with the total photoabsorption cross section ($T_<$ component) calculated by Albert *et al.* (Ref. 7) using a δ-function potential with a Soper mixture of exchange forces. The scale of the calculated cross section has been reduced by a factor of 4 to facilitate comparison with the measurement. Ground state transitions appear to account for all of the $T_<$ strength in the neutron channel below about 17 MeV and about half of the calculated $T_<$ strength above 19.5 MeV. The state of about 17.3 MeV corresponds closely in energy and single-particle composition to a state predicted by the calculation of Fraser *et al.* (Ref. 5).

ly the same (-10.8 vs -10.2 MeV), decays via the neutron and proton channels should occur with about equal probability.

A minimum centered at 16.2 MeV in the theoretical curve is also seen in the experimental curve over this energy region. Above 19.5 MeV there is remarkable agreement between the shapes of the experimental and theoretical results. Between 17 and 19.5 MeV, the strong peaking predicted by the calculation is not seen to be reflected in the data. The ground state cross section is roughly $\frac{1}{8}$ the level of the theoretical result. From this we can conclude that the $T_<$ strength in the neutron channel is approximately four times that exhausted by the ground state channel alone. Similarly, by assuming that the branching ratio

$$\sigma(\gamma,p_{\text{tot}})/\sigma(\gamma,n_{\text{tot}})\sim 1\ ,$$

it is seen that the ground state channel makes up most of the $T_<$ strength below 17 MeV and about one-half of the $T_<$ strength above 19.5 MeV in the neutron channel.

Also shown in Fig. 5 is a single state (dashed line) predicted by Fraser *et al.*[5] also using a δ-function interaction with a Soper exchange mixture and an 8 MeV well. The excited state of the ^{15}N nucleus was interpreted as a one-particle-two-hole state in ^{16}O. The position of this state (17.5 MeV) is in good agreement with the position of a well defined state observed in both the ground state and total photoneutron cross sections (see Fig. 6). In addition, the predicted single particle composition of the state ($s/d=0.44$) is consistent with the value of $a_2/a_0=-0.7$ obtained experimentally over this energy region.

A comparison between the ground state and total photoneutron cross sections (Fig. 6) shows that the two measurements are in good agreement up to 15 MeV. The agreement between ground state and nonground state measurements below 15 MeV has been predicted by Patrick *et al.*[19] and can be deduced from the linearity of the measurement of average neutron energy as a function of excitation energy below 15 MeV made by Jury *et al.*[11] Above 15.5 MeV, it is seen that only about one-third of the (γ,n_{tot}) cross section results in transitions to the ground state. This is consistent with the calculations of Brown *et al.*[20] which show that for the case of ^{16}O, one-particle-one-hole transitions resulting in an excited state configuration for the residual nucleus make up 66.5% of the total dipole strength in the giant resonance, the majority of this being transitions of the type $p_{3/2}{}^{-1}d_{5/2}$.

Figure 7 shows the mirror reaction ^{15}O$(\gamma,p_0)^{14}$N obtained by detailed balance from a measurement by Harakeh *et al.*,[10] our result for the differential cross section at 90° obtained using the coefficients extract-

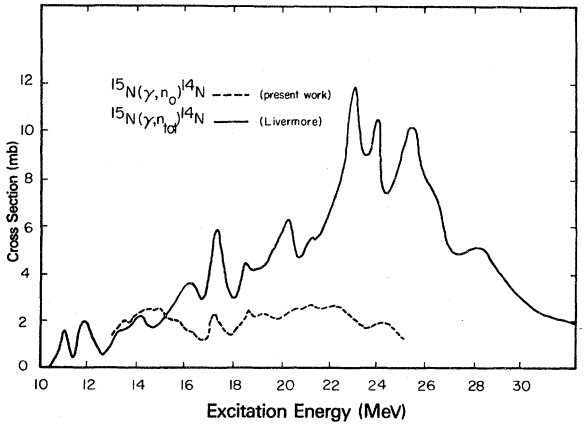

FIG. 6. The present results are compared with the total photoneutron measurement of Jury *et al.* (Ref. 11). The state at 17.3 MeV is seen in both measurements, as is a similar peak at 18.4 MeV. The two measurements agree to within the quoted experimental error (not shown) for excitation energies below about 15 MeV. The ground state cross section shows little evidence of the GDR.

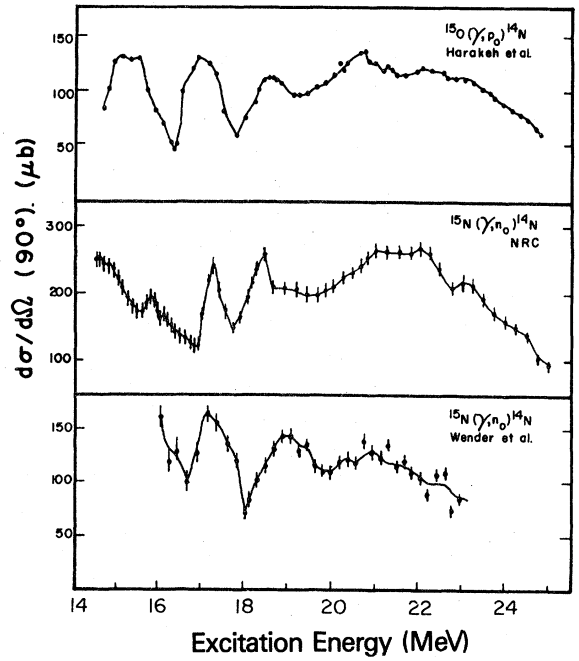

FIG. 7. The differential cross section at 90° was obtained from the measured angular distribution coefficients and is shown along with results for the mirror reaction ^{15}O$(\gamma,p_0)^{14}$N (Ref. 10) and with the identical photoneutron reaction by applying detailed balance to the results of Ref. 12 on the ^{14}N$(n,\gamma_0)^{15}$N reaction. The cross sections display similar features. However, the vertical scale on the present measurement is larger than the other two (also note the suppressed zero).

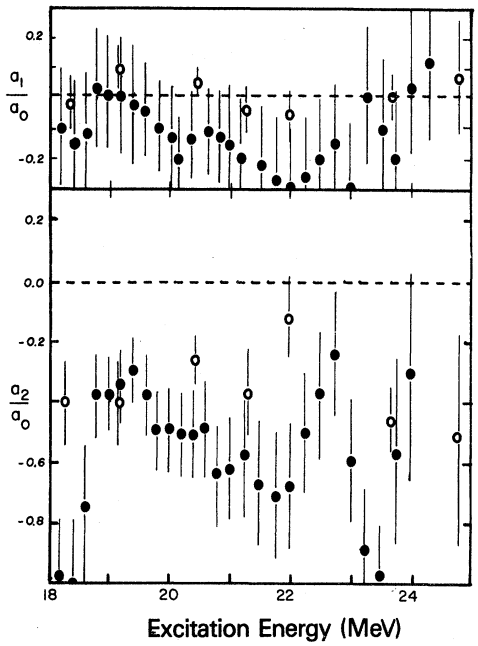

FIG. 8. A comparison of the angular distribution coefficients from the present work with those from Ref. 12 (open circles). Error bars represent fitting errors.

ed from a fit to eight angles, and the result of Wender *et al.*[12] obtained by detailed balance from a measurement of the inverse reaction. Our measurement indicates the presence of at least three well defined states below 19 MeV at 15.8, 17.3, and 18.4 MeV excitation energy. The shapes of the three curves are very similar, however our cross section is somewhat higher than that obtained by Wender. The general trend of the angular distribution coefficients is reproduced by both measurements (see Fig. 8). The plot of the a_1/a_0 coefficients shows, on an expanded scale, a generally small near-zero value (within error bars) except near 22 MeV where there appears to be a systematic deviation from zero and hence the possibility of interfering $E2$ or $M1$ amplitudes.

VI. CONCLUSION

The cross section for the reaction $^{15}N(\gamma,n_0)^{14}N$ has been measured relative to the theoretical cross section for the deuteron calculated by Partovi, Fabian, and Arenhovel [and confirmed experimentally by Ahrens *et al.*[21]]. The single particle nature of the reaction (in particular that of a state at 17.3 MeV) has been deduced on the basis of measured angular distribution coefficients and found to be in agreement with that predicted by Fraser *et al.*[5] The analysis of the Legendre coefficients was based on the assumption that interfering $E2$ and $M1$ amplitudes were small, an assumption confirmed by our values of a_1/a_0 which were found to be zero within the precision of the measurement over most of the region of excitation energy studied. The ground state cross section can be interpreted on the basis of $p_{1/2}{}^{-1}d_{3/2}$ single-particle transitions with a small admixture of $p_{1/2}{}^{-1}s_{1/2}$ strength. Isospin fragmentation of the GDR was observed by comparing the (γ,n_{tot}) measured by Jury *et al.*[11] with the present measurement which was exclusively $T_<$.

ACKNOWLEDGMENTS

We thank Mr. Alex Nowak and the staff of the National Research Council of Canada (NRCC) Electron Linear Accelerator Laboratory for their assistance in the data-taking stage of this work. This work was supported in part by the Natural Sciences and Engineering Research Council of Canada.

[1]V. Gillet and H. Vinh Mau, Nucl. Phys. 54, 321 (1964).
[2]F. W. K. Firk, Annu. Rev. Nucl. Sci. 20, 39 (1970).
[3]*Photonuclear Reactions,* edited by E. G. Fuller and E. Haywood (Dowden, Hutchinson, and Ross, Stroudsburg, Pennsylvania, 1976), Vol. 2.
[4]M. Marangoni and A. Saruis, Nucl. Phys. A132, 649 (1969).
[5]R. F. Fraser, R. K. Garnsworth, and B. M. Spicer, Nucl. Phys. A156, 489 (1970).
[6]R. F. Barrett, R. F. Fraser, and P. P. Delsanto, Phys. Lett. 40B, 32 (1972).
[7]D. J. Albert, A. Nagl, J. George, R. F. Wagner, and H. Überall, Phys. Rev. C 16, 503 (1977).
[8]H. R. Kissener and R. A. Eramzhian, private communication.
[9]J. W. Jury, B. L. Berman, D. D. Faul, P. Meyer, and J. G. Woodworth, Phys. Rev. C 21, 503 (1979).
[10]M. H. Harakeh and P. Paul, Phys. Rev. C 12, 1410 (1975).
[11]J. W. Jury, B. L. Berman, J. G. Woodworth, M. N. Thompson, R. E. Pywell, K. G. McNeill, Phys. Rev. C 26, 777 (1982).
[12]S. A. Wender, H. R. Weller, N. R. Roberson, D. R. Tilley, and R. G. Seyler, Phys. Rev. C 25, 89 (1982).
[13]J. W. Jury, C. K. Ross, and N. K. Sherman, Nucl. Phys. A337, 503 (1980).
[14]W. Fabian and H. Arenhovel, private communication.
[15]F. Partovi, Ann. Phys. (N.Y.) 27, 29 (1964).
[16]*Data Reduction and Error Analysis for the Physical Sciences,* P. R. Bevington (McGraw-Hill, New York,

1969).
[17]R. W. Carr and J. E. E. Baglin, Nucl. Data Tables 10, (1971).
[18]D. J. Albert, J. George, and H. Überall, Phys. Rev. C 16, 2452 (1977).
[19]B. H. Patrick, E. M. Bowey, and E. G. Muirhead, Nucl. Phys. G2, 751 (1976).
[20]G. E. Brown, L. Castillejo, and J. A. Evans, Nucl. Phys. 22, 1 (1961).
[21]J. Ahrens, H. P. Eppler, A. Gimm, M. Kröning, P. Riehn, H. Wäffler, A. Zieger, and B. Ziegler, Phys. Lett. 52, 49 (1974).